

Raman scattering characterization of gel-derived titania glass

P. P. LOTTICI, D. BERSANI, M. BRAGHINI*, A. MONTENERO*

*Dipartimento di Fisica and Consorzio INFN, and *Istituto di Strutturistica Chimica, Università di Parma, Viale delle Scienze, 43100 Parma, Italy*

The preparation by the sol–gel method of bulk vitreous TiO_2 is reported and its transformation both by controlled thermal treatment and by laser-induced heating in the anatase and rutile crystalline forms is studied by Raman spectroscopy. The results are compared with those existing for amorphous TiO_2 thin films. The dependence of the Raman frequencies and linewidths on the incident laser power is presented and the Raman spectrum of the brookite (a third naturally occurring form of TiO_2) is also reported as a comparison.

1. Introduction

Since the development of the sol–gel technique, great attention has been paid to glasses in bulk and thin-film form with mixed TiO_2 – SiO_2 composition [1–6]. These glasses are important because of their very low thermal expansion and because of the possibility of obtaining a desired expansion coefficient by changing the $\text{TiO}_2/\text{SiO}_2$ ratio. For these reasons, little or no attention has been paid to pure TiO_2 (titania) in its amorphous form. Moreover, titanium dioxide has been classified by Zachariasen [7] as an intermediate or network-modifying oxide as it does not appear to form a glass by itself.

Much work has been reported on titania films on different substrates. Pure titania films were deposited by Perry and Pulker [8] by physical methods with the aim of improving the abrasion resistance of the substrate. Hadj *et al.* [9] prepared coatings of pure TiO_2 and pure ZrO_2 . They obtained homogeneous films with high refractive index and found that the crystallization of the TiO_2 films did not imply any variation in their optical properties. Amorphous thin films obtained from sputtering techniques [10] or by electrochemical synthesis [11] have been recently reported. Two papers on gel-derived titania were presented at the VI International Workshop on Glasses and Ceramics from Gels, Seville: Bahtat *et al.* [12] studied the thermal evolution of thin films with composition ranging from pure TiO_2 to $>66\%$ SiO_2 , whereas Pernice *et al.* [13] were interested on the crystallization kinetics of the gels.

Different methods (interference-enhanced Raman scattering [14], polarization analysis [15], waveguide Raman spectroscopy [12]) have been proposed to characterize thin films of TiO_2 by Raman scattering techniques, in order to extract the spectrum of the film with respect to the Raman signal of the substrate. Here we are interested to study, by means of Raman spectroscopy, the phase transformations occurring during heat treatments in bulk gel-derived TiO_2 .

2. Preparation and characterization

Titanium isopropylalkoxide (TIPT) was used as precursor compound for the sol–gel process. To slow down the reaction hydrolysis, which is too fast when exposed to the air, the precursor was modified as proposed by Budd and Payne [16], i.e. by changing the isopropyl group by methoxyethoxy groups. The reactions were conducted under a purified nitrogen atmosphere. During the substitution reaction, the TIPT and the methoxyethanol were mixed in a Schlenk apparatus and the isopropylalcohol distilled at 120°C . The obtained amber solution contains the tetramethoxyethoxytitanium (TMET). The reaction is controlled by nuclear magnetic resonance spectroscopy [17]. The solution stored under nitrogen was hydrolysed in acidic conditions and a bulk gel was obtained. The gel was dried at 110°C for 24 h and then powdered.

Differential calorimetric analysis (Perkin Elmer DSC 7) and thermogravimetric analysis (Perkin Elmer TGA 7) were carried out on the pure TiO_2 gel dried at 110°C (Fig. 1). Both analyses were made in air with a heating rate of $10^\circ\text{C min}^{-1}$. DTA measurements were performed by Pernice *et al.* [13] on TiO_2 and ZrO_2 gels up to temperatures higher than 800°C . They observed two peaks at ≈ 400 and 800°C , attributed to anatase and rutile crystallization, respectively. Yoko *et al.* [18] found a DTA peak at 258°C , due to the combustion of the organic substances contained in the gel, a peak at 468°C ascribed to the crystallization of the anatase, and a very feeble change at about 720°C attributed to the beginning of the transformation to rutile. In the case of TiO_2 films deposited on Nesa glass, they found the anatase peak at 500°C . Our TGA and DSC measurements show three transformations at about 290 , 360 and 490°C . Whereas the first exothermic peak is attributed to the combustion of the organics present in the bulk gel, the peak at 360°C is due to the formation of anatase, as has been confirmed by the X-ray diffraction spectra. X-ray diffraction on a

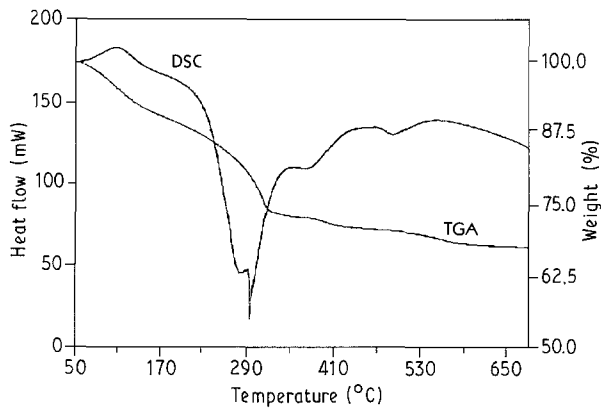


Figure 1 Differential calorimetric analysis (DSC) and thermogravimetric analysis (TGA) of TiO_2 gel dried at 110°C .

bulk sample treated at 490°C for 10 min shows only the anatase phase, and we suggest that the 490°C peak could be due to a combustion of high-temperature-resistant organic materials.

After these preliminary thermal analyses, different heat treatments were performed on the powder to study the crystallization processes. The structure of the heat-treated powders was determined by X-ray diffraction using CuK_α radiation at a scan rate of $1^\circ 2\theta \text{ min}^{-1}$. All samples for X-ray diffraction were back-loaded packed-powder specimens. X-ray diffraction patterns taken on powders treated at a heating rate of 100°C h^{-1} are presented in Figs 2 and 3. The

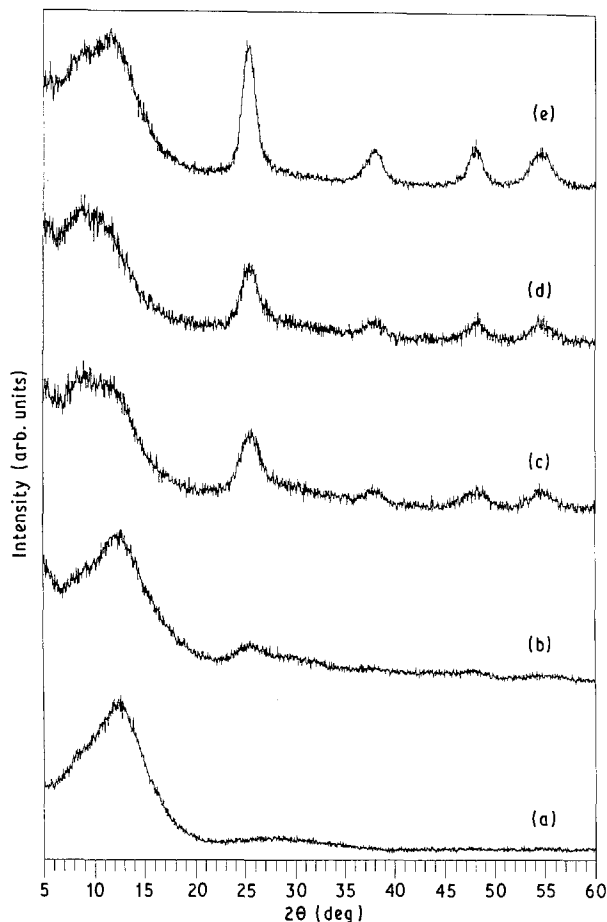


Figure 2 X-Ray diffraction patterns of the heat-treated TiO_2 powder: gels dried at (a) 110°C , (b) 200°C , (c) 250°C , (d) 300°C , (e) 350°C . The transition from vitreous to anatase TiO_2 is shown.

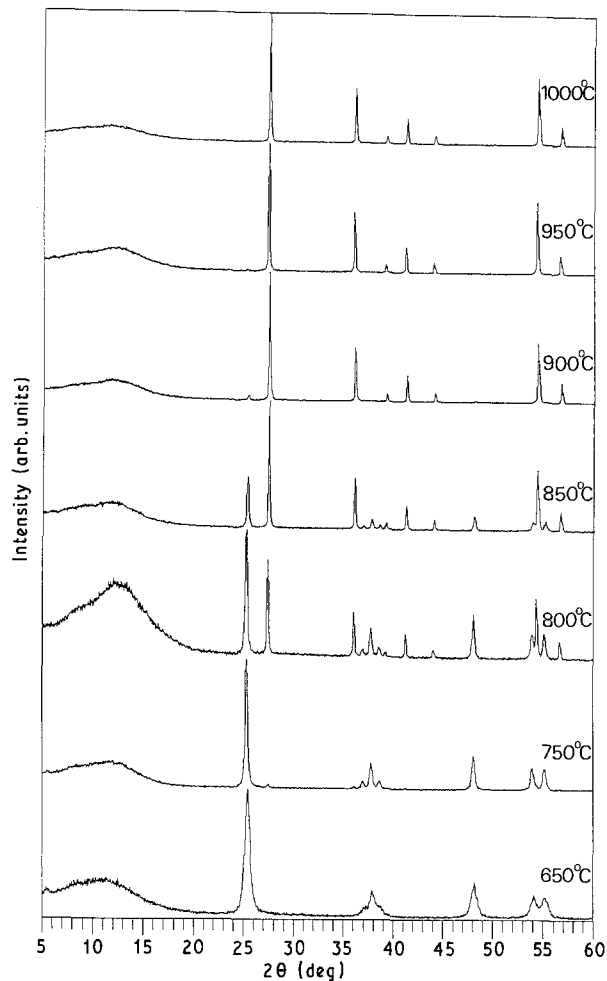


Figure 3 X-Ray diffraction pattern of the heat-treated TiO_2 powder from 650 – 1000°C showing the transformation from anatase to rutile phase.

dried gel powder is amorphous, as indicated by the absence of any crystalline structure (Fig. 2a). Wide crystalline peaks grow at higher temperatures until the treatment is performed at 350°C , where the diffraction peaks of the anatase are clearly resolved (Fig. 2e). The diffraction patterns of samples treated up to 1000°C (Fig. 3) indicate that both crystalline TiO_2 forms (anatase and rutile) are present, with increasing rutile content, up to a complete rutile phase. The broad peak at $2\theta \approx 10^\circ$ – 15° has been attributed to the vitreous titania phase: its increased presence in the X-ray diffraction on the powder treated at 800°C could indicate an amorphization of titanium dioxide in the vicinity of the anatase–rutile phase transformation point as suggested by Bobovich and Tsentser [19]. This point, however, deserves further investigation.

In Fig. 4 we show the X-ray diffraction spectra of powders heated to 750°C and then held at that temperature for up to 3 h. We observe that at this temperature the rutile phase grows with time: thermal treatments at lower temperatures show no modification in the pure anatase spectrum, apart from some better resolution of the peaks.

3. Raman scattering measurements

The Raman spectra were taken both on powders in capillary tubes and on pellets. The exciting light was

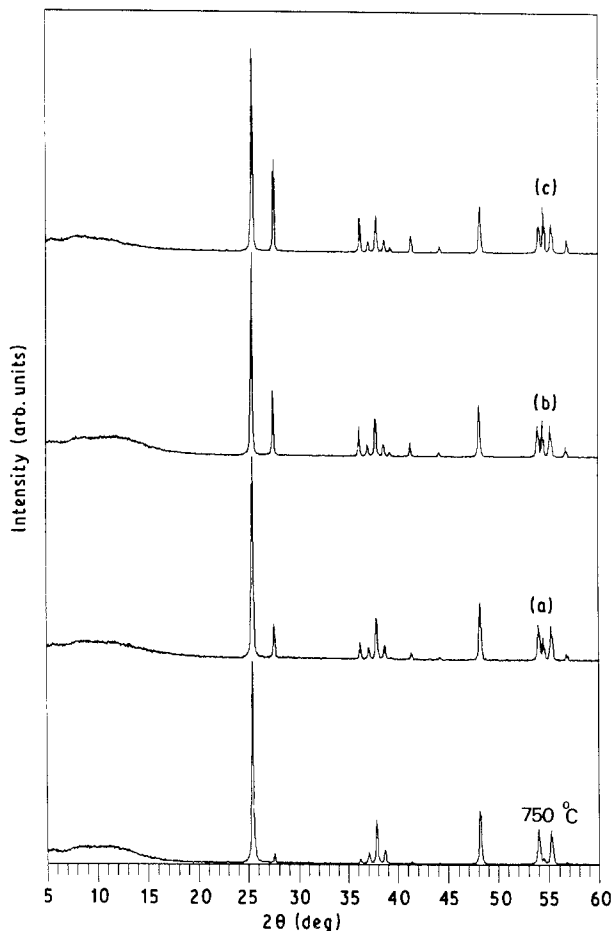


Figure 4 X-Ray diffraction patterns of the powder treated at 750 °C for (a) 1 h, (b) 2 h and (c) 3 h. The rutile peaks grow with annealing time.

obtained from a Coherent 2020 model cw Ar⁺ laser operating at 514.5 nm. The spectra were collected in a nearly back-scattering geometry by a SPEX 1403 double monochromator equipped with a Hamamatsu R 4362-2 photomultiplier and a photon counting system. The spectral resolution was set at about 0.5 cm⁻¹. The spectra were taken on the same powdered samples used for the X-ray diffraction measurements at power levels ≈ 40–50 mW.

The Raman spectrum of the dried gel TiO₂ (which is shown later in Fig. 9a) shows no features, apart from the usual low-frequency quasi elastic scattering, thus confirming its amorphous nature. The absence of Raman features in the amorphous form of TiO₂ agrees with a similar conclusion of Arsov *et al.* [11] about the Raman spectrum of thin films of amorphous titanium dioxide obtained by electrochemical synthesis.

The Raman spectra of the heat-treated powders (Fig. 5) up to 350 °C confirm the gradually occurring change from vitreous TiO₂ to anatase: this change is followed through the evolution of the most intense anatase peak in the region 145–160 cm⁻¹. The size of the microcrystals in the crystallization process should grow with increasing temperature and annealing time. The Raman peaks should then display smaller line-widths (FWHM) due to an increase in the correlation length of the vibrations and increasing intensity due to greater concentrations of anatase phase. The FWHM

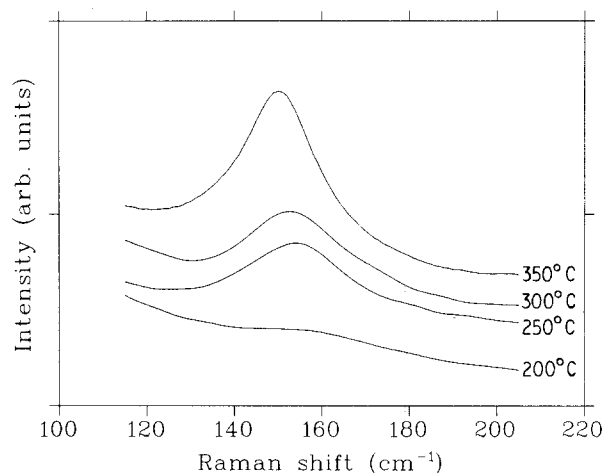


Figure 5 Raman spectra of the most intense anatase peak showing the transition from glass to anatase on the samples whose XRDs are shown in Fig. 2b–e. The Raman spectrum of the dried gel is reported in Fig. 9. The Raman band shifts from ≈ 159 cm⁻¹ to 149 cm⁻¹. The corresponding anatase peak is at 144 cm⁻¹ (see Fig. 6).

of the anatase peak decreases from about 28 cm⁻¹ to 15 cm⁻¹ for the samples treated at 200 and 350 °C, respectively. We notice, however, that with increasing temperature the anatase peak shifts to lower frequencies: this red-shift is opposite to the well-known blue-shift occurring in the amorphous to microcrystalline transitions in tetrahedrally bonded silicon and germanium [20, 21]. This effect in TiO₂ has not been explained: it could be a size-induced pressure effect on the vibrational modes. The lower the microcrystallite size, the higher are the pressure and the Raman frequencies.

The Raman spectra corresponding to the transition from anatase to rutile are reported in Figs 6 and 7. The Raman spectrum of the anatase phase (Fig. 6) shows peaks at 144, 197, 399, 515, 638 cm⁻¹ which agree with the Raman frequencies on anatase single crystals reported in the literature [22, 23]. The three bands at 638, 197, 144 cm⁻¹ are assigned to E_g modes and the band at 399 cm⁻¹ to the B_{1g} mode. The band at 515 cm⁻¹ is a doublet of A_{2g} and B_{1g} modes. The weak band at ≈ 800 cm⁻¹ has been attributed to the first overtone of the 399 cm⁻¹ peak [23]. The full width at half maximum (FWHM) of the 144 cm⁻¹ peak for the sample heated at 700 °C is 7 cm⁻¹, exactly as the FWHM reported for monocrySTALLINE anatase [22].

According to Ohsaka *et al.* [24] and to Balachandran and Eror [23], in the commercial anatase powder, the anatase to rutile transformation does not occur even at 800 °C. After a heat treatment at 750 °C for 3 h, we observe the growth of the rutile phase, both by X-ray diffraction (Fig. 4) and Raman scattering (Fig. 8). As already mentioned, no evidence of the rutile phase is observed for long treatments at lower temperatures: our results on a gel-derived powder thus indicate that the rutile phase is obtained from the anatase at temperatures below 800 °C.

After the complete anatase to rutile transformation (Fig. 7), the Raman spectrum of rutile reproduces the existing literature data [25–27] (peaks at 143, 447, 612 cm⁻¹, a broad band at 826 cm⁻¹ and a strong

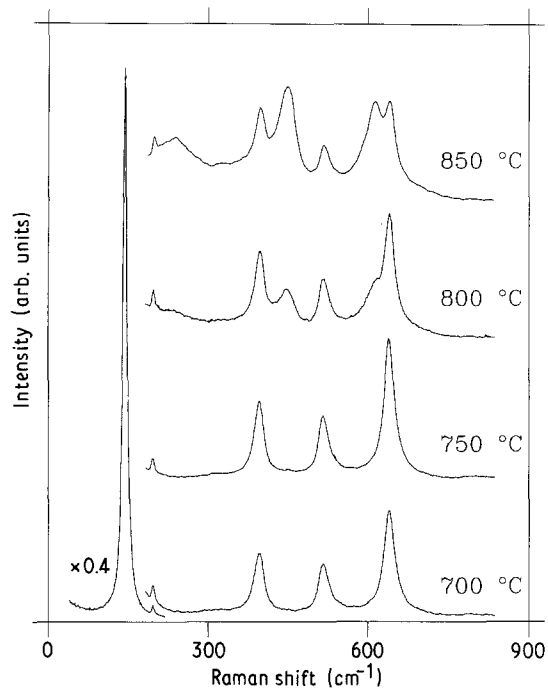


Figure 6 Raman spectra of the heat-treated TiO_2 powder. Starting from the spectrum on the powder treated at 800°C the rutile peaks are clearly visible. The most intense peak of anatase at 144 cm^{-1} is reported only for the spectrum at 700°C , with its intensity reduced by a factor of 2.5. The corresponding XRD spectra are shown in Fig. 3.

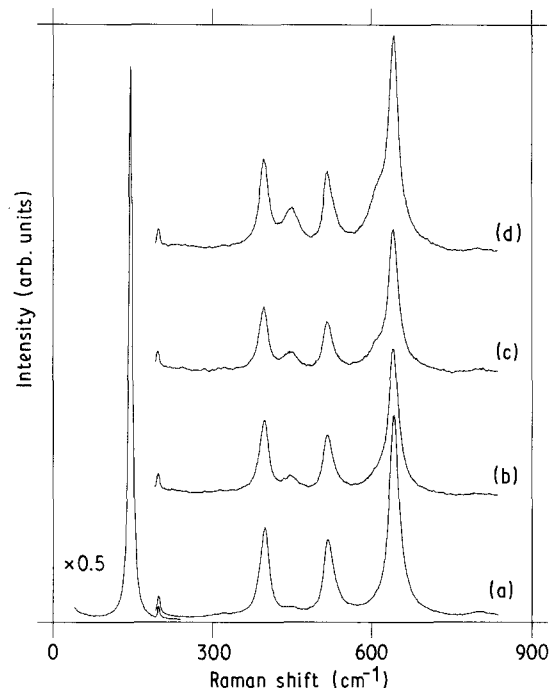


Figure 8 Raman spectra of the powder treated at (a) 750°C , (b) for 1 h, (c) 2 h and (d) 3 h. The rutile peaks grow with annealing time. The most intense peak of anatase at 144 cm^{-1} is seen only once with its intensity reduced by a factor of 2. The corresponding XRD spectra are shown in Fig. 4.

combination band at 235 cm^{-1}). Thermal treatments at temperatures higher than 1000°C do not change the X-ray diffraction and the Raman scattering.

In addition to these low laser intensity measurements, Raman spectra were taken at increasing laser power by focusing the laser beam by means of a spherical lens on an as-prepared dried powder, thus

inducing a thermal crystallization of the sample. Different runs on different positions on the pellets were made and the reproducibility of the results has been largely verified. Fig. 9 shows the transformation of the Raman spectrum. The dried gel shows no Raman spectrum, as already mentioned. As the laser power is increased, the anatase features appear, with increasing

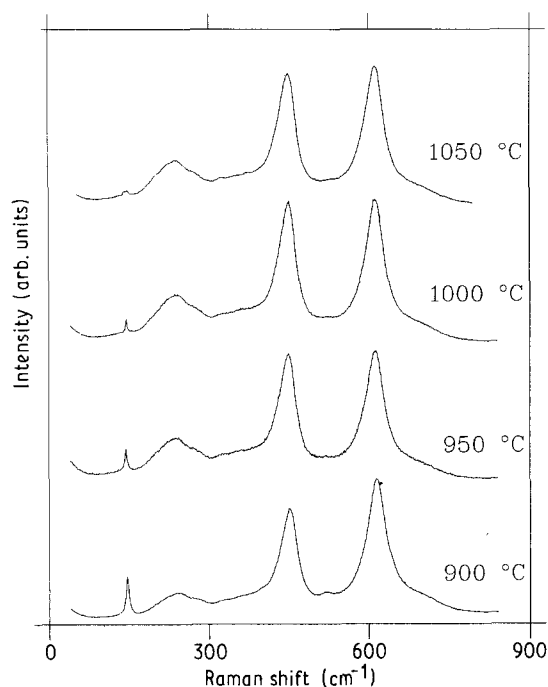


Figure 7 Raman spectra of the heat-treated TiO_2 powder. A complete rutile spectrum is found at $1000\text{--}1050^\circ\text{C}$. The corresponding XRD spectra are shown in Fig. 3.

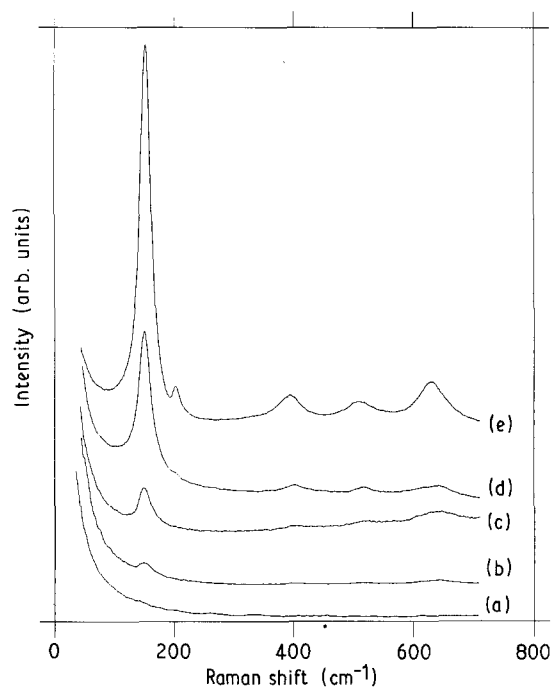


Figure 9 Raman spectra taken with increasing laser power of the 514.5 nm argon line on the dried gel powder. (a) 40 mW ; (b) 150 mW ; (c) 250 mW ; (d) 450 mW ; (e) 750 mW . The spectrum changes from the vitreous TiO_2 (a) to pure anatase (e).

intensity, up to the pure anatase spectrum which is obtained at a power of approximately 750 mW on a spot of about 50 μm diameter. These Raman spectra should be compared with the spectra shown in Fig. 5, which were taken at low laser power: now the increasing laser intensity causes some heating of the sample and the red-shift of the main anatase peak during crystallization is obscured by a blue-shift of the peak with temperature, as will be discussed below.

The spectrum of the laser-induced pure anatase phase (Fig. 9e) is the same, apart from the temperature shifts of the Raman peaks, as that obtained on the heat-treated powder at 750 $^{\circ}\text{C}$ (Figs 6 and 8a) whose X-ray diffraction spectrum has been shown in Fig. 3. There is no co-existence of anatase and rutile phases at beam powers up to ≈ 1000 mW, as no signature of the rutile Raman bands as shoulders of the anatase peaks have been observed, contrary to what was suggested by Balachandran and Eror [23]. This fact corresponds to the absence of any rutile structure by heat treatment of the vitreous powder below 750 $^{\circ}\text{C}$.

Raman measurements at increasing laser power on the pure anatase phase show that the anatase peaks at 144 and 197 cm^{-1} shift to higher frequencies, whereas the other modes shift to lower frequencies. This power-temperature dependence agrees with published data [22] for four modes in anatase. We add to these results the power dependence of the doublet at 515 cm^{-1} which is shown in Fig. 10. In the same figure, we also report the blue-shift of the most intense

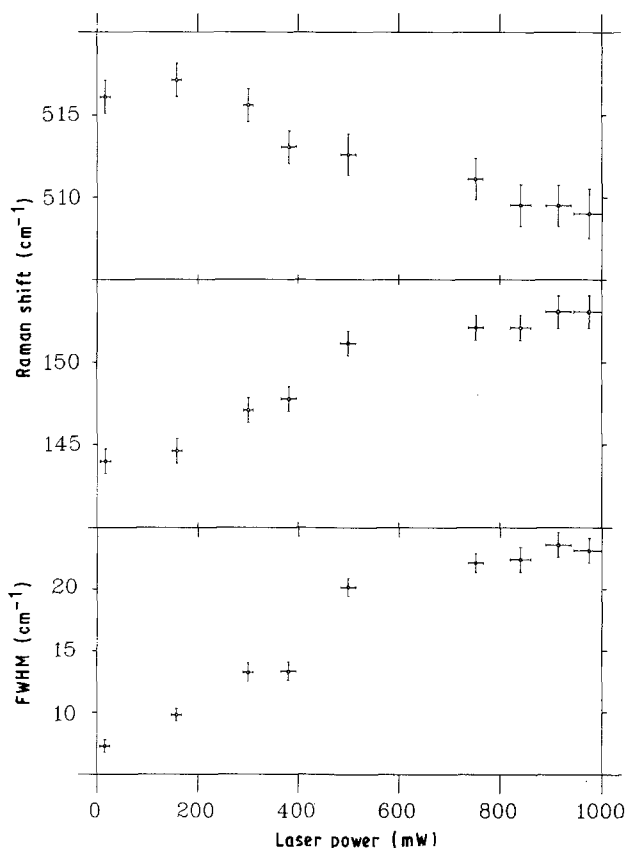


Figure 10 Dependence of the anatase 515 cm^{-1} $A_{2g} + B_{1g}$ mode and of the 144 cm^{-1} E_g mode frequencies on the incident laser power. The FWHM of the 144 cm^{-1} peak is shown at the bottom. Approximate error bars are given.

anatase peak and its FWHM power-temperature dependence. The reported values agree with the data on single anatase crystals and suggest that the temperature reached at 1000 mW is about 700 $^{\circ}\text{C}$. We tried to test the temperature using the ratio of Stokes to Antistokes intensities but without useful results. Measurements at laser-beam power higher than 1000 mW result in surface damage. The coexistence between the anatase and rutile structure is observed only by turning down to low light intensity. Different rutile to anatase ratios are formed by different thermal cycling from high to low power (Fig. 11). A final complete rutile phase is obtained for laser power above some threshold which may be estimated at about 1200 mW.

After the complete anatase to rutile transformation, the Raman spectrum of rutile taken at low power (40 mW) reproduces the spectrum of the rutile powder obtained by the heating process. At higher laser power (i.e. temperatures), the rutile peaks shift in energy: our data extend the results given by Samara and Peercy [28] on the temperature dependence of the rutile Raman frequencies. The peaks at 143 cm^{-1} (B_{1g}) and at 612 cm^{-1} (A_{1g}) slightly shift to higher frequencies, whereas the E_g mode at 447 cm^{-1} decreases its frequency with increasing power down to 428 cm^{-1} and the combination band shifts from 235 cm^{-1} up to 260 cm^{-1} (Fig. 12).

From the relative intensities of the Raman peaks, we notice that in the commercial rutile (whose spectrum is shown in Fig. 13) the 143 cm^{-1} peak has a higher intensity than in the heat-treated powder at 1000 $^{\circ}\text{C}$ or in the laser-heated (at high power for long time) rutile powder. In gel-derived anatase the relative intensities of the peaks agree with the published data on single crystals [23].

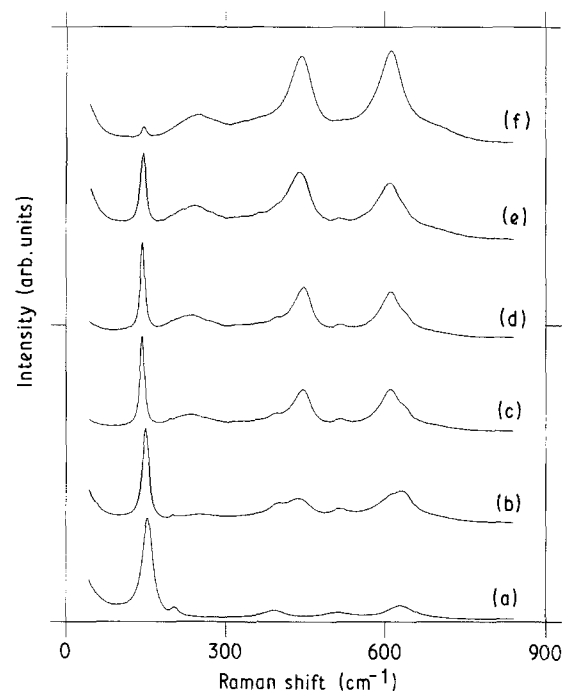


Figure 11 Raman spectra taken with increasing laser power on the TiO_2 powder. The coexistence between anatase and rutile is obtained by different thermal cycling by reaching maximum power from (a) 900 mW to (b) 1200 mW.

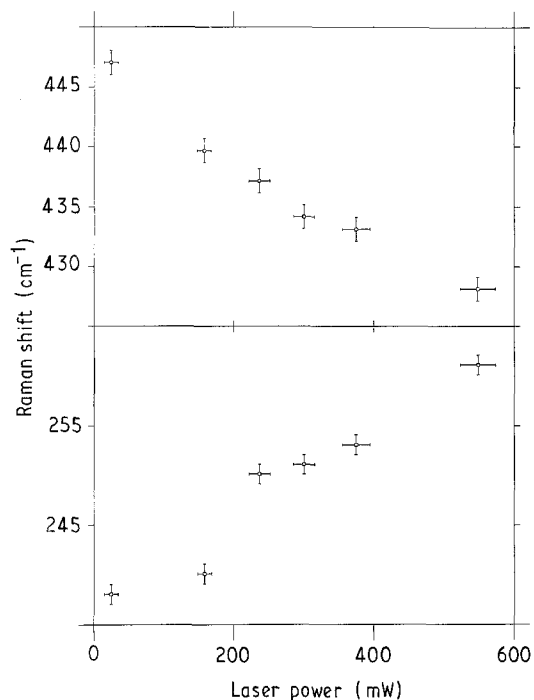


Figure 12 Dependence of the rutile 235 cm^{-1} combination band and of the $447\text{ cm}^{-1} E_g$ mode frequencies on the incident laser power. Approximate error bars are given.

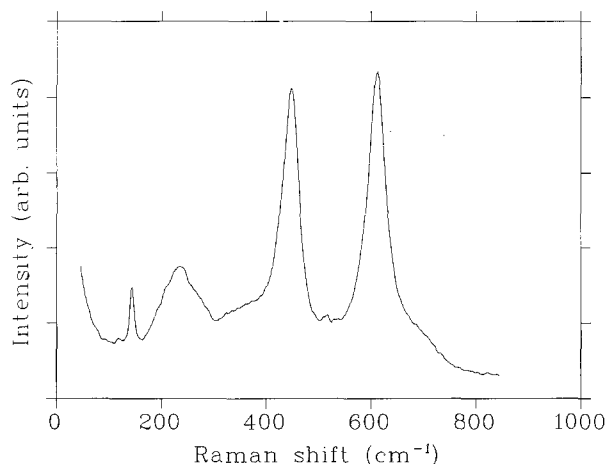


Figure 13 Raman spectrum of commercial rutile.

Hsu *et al.* [10, 29] prepared amorphous titania films by ion-beam sputtering, ion-assisted deposition and electron-beam techniques: they followed the thermally induced and the laser annealing crystallization by Raman scattering. They observed amorphous to crystalline transformations (both anatase and rutile depending on the annealing temperatures and heating time) and a second transition, anatase to rutile at about 900°C . These results depend on the substrate temperature during deposition and are not clearly reproducible. Only for an amorphous coating (electron-beam deposited) did they obtain first the crystallization into the anatase structure for annealing temperatures up to 700°C and then the anatase to rutile transformation for annealing temperatures above 900°C . Our results on bulk amorphous titania, however, confirm that for heat treatment and laser-induced heating the phase transformation sequence is amorphous to anatase and anatase to rutile.

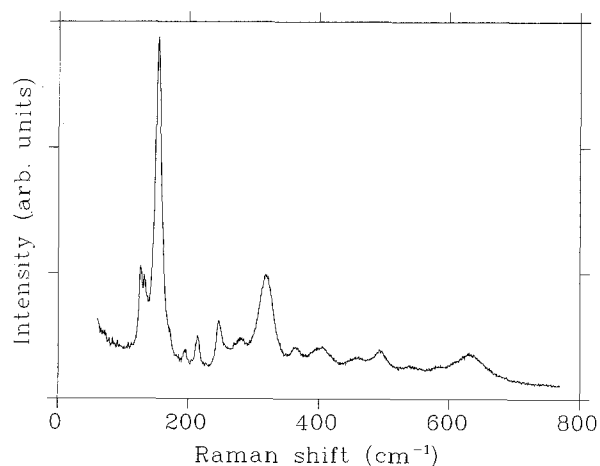


Figure 14 Raman spectrum of natural brookite, found by one of the authors (D.B.) on Mount Bregaceto, Genova, Italy.

Recently, a transformation to the brookite third phase of TiO_2 has been suggested on electrochemically prepared titania films [11]. We report the Raman spectrum of brookite (Mount Bregaceto, Genova, Italy) in Fig. 14. The Raman frequencies agree with those obtained by Arkhipenko *et al.* [30] but we found additional features and some directional dispersion of the peaks according to the scattering geometry used. We have not observed in all our Raman spectra on titanium dioxide, after various laser-heating treatments, any feature which could be attributed to a brookite-like phase.

A more detailed discussion of the Raman scattering in brookite crystals with peak symmetry assignments will be published in the near future.

4. Conclusions

The sol-gel production of titania whose vitreous nature has been confirmed by X-ray diffraction and Raman scattering is reported. We have followed the glass to anatase and to rutile (at $\approx 750^\circ\text{C}$) transformations both by heat treatment and by laser-induced crystallization. Raman scattering reveals an unusual red-shift of the most intense anatase peak with thermal treatment towards crystallization. We have found that the crystalline structure after the first transformation is definitely anatase with no evidence of rutile microcrystals in the amorphous powder or of different brookite-like crystalline phases at high temperatures or laser powers. Raman scattering on laser-heated samples gave qualitative information on the temperature dependence of the Raman frequencies of both anatase and rutile.

Acknowledgements

This work was partially supported by the CNR (National Research Council under the MSTA Project, Materiali Speciali per Tecnologie avanzate). We thank Professor M. P. Fontana for helpful discussions and Professor C. Razzetti and Dr G. Antonioli for assistance in the Raman experimental work.

References

1. B. E. YOLDAS, *J. Non-Cryst. Solids* **38/39** (1980) 81.
2. C. J. BRINKER and M. S. HARRINGTON, *Solar Energy Mater.* **5** (1981) 159.
3. T. HAYASHI, T. YAMADA and H. SAITO, *J. Mater. Sci.* **18** (1983) 3137.
4. C. J. R. GONZALES-OLIVER, P. F. JAMES and H. RAWSON, *J. Non-Cryst. Solids* **48** (1982) 129.
5. S. SAKKA, K. KAMIYA, K. MAKITA and Y. YAMAMOTO, *ibid.* **63** (1984) 223.
6. C. ZHU, L. HOU, F. GAN and Z. JIANG, *ibid.* **63** (1984) 105.
7. W. H. ZACHARIASEN, *J. Amer. Chem. Soc.* **54** (1932) 384.
8. A. J. PERRY and K. PULKER, *Thin Solid Films* **124** (1985) 323.
9. B. HADJ, R. SEMPERE, J. DHALIPPOV, *J. Non-Cryst. Solids* **82** (1986) 417.
10. L. S. HSU, R. SOLANKI, G. J. COLLINS and C. Y. SHE, *Appl. Phys. Lett.* **45** (1984) 1065.
11. Lj. D. ARSOV, C. KORMANN and W. PLIETH, *J. Raman Spectrosc.* **22** (1991) 573.
12. M. BAHTAT, J. MUGNIER, C. BOVIER and J. SERUGHETTI, in "Proceedings of the VI International Workshop on Glasses and Ceramics from Gels", Seville (1991) AP5.
13. P. PERNICE, A. ARONNE, A. MAROTTA and A. BURI, *ibid.*, AP 41.
14. R. J. NEMANICH, C. C. TSAI and G. A. N. CONNELL, *Phys. Rev. Lett.* **44** (1980) 273.
15. G. J. EXARHOS, *J. Chem. Phys.* **81** (1984) 5211.
16. K. D. BUDD and D. A. PAYNE, in "Materials for Non-Linear and Electro-Optics 1989", Institute of Physics Conference Series Number 103, Edited by M. H. Lyons (Institute of Physics, Bristol and New York, 1989) p. 13.
17. S. D. RAMAMURTHI and D. A. PAYNE, *J. Amer. Ceram. Soc.* **73** (1990) 2547.
18. T. YOKO, K. KAMIYA and S. SAKKA, *Yogyo Kyokai-Shi* **95** (1987) 2.
19. Y. S. BOBOVICH and M. Y. TSENTSER, *Opt. Spectrosc. (USSR)* **62** (1987) 563.
20. H. RICHTER, Z. P. WANG and L. LEY, *Solid State Commun.* **39** (1981) 625.
21. S. HAYASHI, M. ITO and H. HANAMORI, *ibid.* **44** (1982) 75.
22. T. OHSAKA, *J. Phys. Soc. Jpn* **48** (1980) 1661.
23. U. BALACHANDRAN and N. G. EROR, *J. Solid State Chem.* **42** (1982) 276.
24. T. OHSAKA, S. YAMOKA and O. SHIMOMURA, *Solid State Commun.* **30** (1979) 345.
25. S. P. S. PORTO, P. A. FLEURY and T. C. DAMEN, *Phys. Rev.* **154** (1967) 522.
26. M. NICOL and N. Y. FONG, *J. Chem. Phys.* **54** (1971) 3167.
27. Y. MARA and M. NICOL, *Phys. status solidi (b)* **94** (1979) 317.
28. G. A. SAMARA and P. S. PEERCY, *Phys. Rev. B* **7** (1973) 1131.
29. L. S. HSU, R. RUJKORAKARN, J. R. SITES and C. Y. SHE, *J. Appl. Phys.* **59** (1986) 3475.
30. D. K. ARKHIPENKO, Y. S. BOBOVICH and M. Y. TSENTSER, *Zh. Prikl. Spektrosk.* **41** (1984) 304.

*Received 3 January
and accepted 2 June 1992*